Для дослідження були обрані чотири типи гідроксиду. Два з них були отримані виробничим шляхом та застосовуються у електродах лужних акумуляторів. Два інші порошки гідроксидів нікелю були синтезовані за експериментальними методами описаними в сучасних наукових джерелах. Перший гідроксид був синтезований гідролітичним методом із розчину, що містив сіль нікелю та карбамід. Інший синтезований із розчину солі, що містив суміш катіонів нікелю й алюмінію у співвідношенні 4:1 та був осаджений при додаванні концентрованого розчину лугу. У результаті всі обрані порошки гідроксидів нікелю сильно відрізнялись за фізико-хімічними параметрами: структурою, фазовим складом, морфологією. Таким чином, було показано, що спосіб синтезу гідроксиду нікелю, й в свою чергу відмінності у структурі та морфології, значно впливають на електрохімічні та інші фізико-хімічні властивості порошків.

У результаті визначення величини питомої поверхні гідроксидів методом адсорбції барвника були отримані значення в інтервалі від 2,52 м²/г до 15,44 м²/г. Визначені величини питомих поверхонь були використані для розрахунку коефіцієнтів дифузії. У свою чергу, коефіцієнти дифузії були отримані для катодного й анодного процесів, а також розраховане їх середнє значення. Отримані значення коефіцієнтів дифузії протона у твердій фазі коливалися від 9,86·10-15 до 9,87·10-17 см²/с.

Порівняння та аналіз електрохімічних характеристик, значень питомої поверхні порошків та коефіцієнтів дифузії дало змогу рекомендувати застосування гідроксидів.

На додачу були запропоновані можливі механізми, що пояснюють отримані значення визначених величин, а також показано взаємозв'язок поміж структурою, способом отримання порошків та їх фізико-хімічними параметрами

Ключові слова: Ni(OH)₂, гідроксид нікелю, спосіб отримання, циклічна вольтамперометрія, питома поверхня, коефіцієнт дифузії протона

DEFINITION OF THE INFLUENCE OF OBTAINING METHOD ON PHYSICAL AND CHEMICAL CHARACTERISTICS OF NI (OH)$_2$ POWDERS

V. Kotok
PhD, Associate Professor
Department of Processes, Apparatus
and General Chemical Technology*
E-mail: valeriykotok@gmail.com
PhD, Senior Researcher
Competence center
"Ecological technologies and systems"**
V. Kovalenko
PhD, Associate Professor
Department of Analytical Chemistry and Chemical
Technologies of Food Additives and Cosmetics*
E-mail: vadimchem@gmail.com
PhD, Senior Researcher
Competence center
"Ecological technologies and systems"**
*Ukrainian State University of
Chemical Technology
Gagarina ave., 8, Dnipro, Ukraine, 49005
**Vyatka State University
Moskovskaya str., 36, Kirov,
Russian Federation, 610000

1. Introduction

Nickel hydroxide has found wide use in chemical power sources – alkaline batteries [1, 2] and asymmetric supercapacitors [3, 4]. Precipitation of nickel hydroxide with different additives is viewed as one way for the preparation of electrodes for water decomposition [5, 6]. Thin films of nickel hydroxide can be potentially applied as electrochromes in smart windows [7, 8]. Precipitation of nickel hydroxide can be realized through many methods [9], with synthesis conditions varying significantly. Synthesis method and synthesis conditions of Ni(OH)$_2$ have a significant effect on its physico-chemical properties: structure, shape and particle size and composition. Listed properties become defining when choosing a synthesis method of nickel hydroxide for a specific application.

It is known that current-generating reaction (1) which occurs in nickel hydroxide is defined by the speed of proton diffusion through solid phase, Fig. 1.

$$Ni(OH)_2 \leftrightarrow NiOOH + H^+ + \bar{e}. \qquad (1)$$
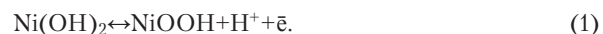
In turn, this speed depends on the proton diffusion coefficient (D_{H^+}) in solid phase [10, 11]. D_{H^+} – primarily depends on the synthesis method used. Also, discharge characteristics depend on another parameter – specific surface area (S_{sp}). Specific surface area characterizes the real current density on a particle and partially – the length of the proton path. This value is also governed by the synthesis method, but can be altered by post-treatment methods [12]. Both these parameters directly influence the capability of Ni(OH)$_2$ for deep discharge and fast charge, even with high currents.
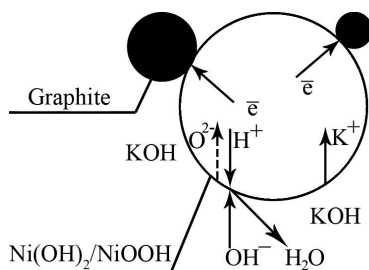
Fig. 1. Schematic depiction of charge (oxidation) of nickel hydroxide particles during the operation of the alkaline battery

As such, it is important to determine the influence of the synthesis method on physico-chemical characteristics of Ni(OH)$_2$, especially on proton diffusion coefficient and specific surface area. Understanding the relation between key factors that determine the effectiveness of Ni(OH)$_2$ in chemical power sources and electrochromic devices would help in forming requirements for synthesis of this compound.

2. Literature review and problem statement

Proton diffusion coefficient can vary significantly between nickel hydroxide samples prepared with different methods. There are also a lot of contractions in data on the proton diffusion coefficient. Literature values of proton diffusion coefficient of Ni(OH)$_2$ vary from 10^{-7} cm^2/s [13] to 10^{-12} cm^2/s, and even up to 10^{-23} cm^2/s [14]. The difference between the minimum and maximum values is nine orders of magnitude.

In addition, the paper [15] describes the dependency of the proton diffusion coefficient on a charge of active material (θ), according to equation (2):

$$D_{H^+} = D_{NiOOH} \left[\theta + (1-\theta) \left(\frac{D_{Ni(OH)_2}}{D_{NiOOH}} \right)^{1/2} \right]^2. \tag{2}$$

Equation (2) assumes that active material is a solid solution, and the member in parentheses is the shift of diffusion particles. For this equation, the values are assumed

$$D_{NiOOH} = 3,4 \cdot 10^{-8} \text{ cm}^2/\text{s}, \ D_{Ni(OH)_2} = 6,4 \cdot 10^{-11} \text{ cm}^2/\text{s}.$$

The paper [15] also describes that changes in the proton diffusion coefficient are independent of proton travel distance, i. e. location of the reaction front. A sharp decrease of the proton diffusion coefficient is explained by proton diffusion resulting from proton hoping from one oxyhydroxide site onto another. During discharge, the oxidation state decreases, resulting in less NiOOH sites, which in turn decreases the proton diffusion coefficient.

In [16], thin films of nickel hydroxide (about 1 μm) deposited onto cathode were used for measuring proton diffusion coefficient. The obtained proton diffusion coefficient values are $4.6 \cdot 10^{-11}$ cm^2/s on discharge and $3.1 \cdot 10^{-10}$ cm^2/s on charge.

The paper [17] described the proton diffusion coefficient of films as $4 \cdot 10^{-13}$ cm^2/s for γ-NiOOH and $1 \cdot 10^{-12}$ см^2/s for β-NiOOH. The films were prepared by cathodic deposition with a thickness of 0.4–2 μm.

Anodically deposited films of active material with a thickness of 10 μm showed the diffusion coefficient within $(5\pm0.6)-(10\pm3) \cdot 10^{-12}$ cm^2/s [18]. The stepwise potential change method with a potential step of 1.21 V was used in experiments.

The stepwise potential change method was also used to the measure proton diffusion coefficient of nickel hydroxide films (about 1 μm), which resulted in the value of $2-5 \cdot 10^{-8}$ cm^2/s [15]. The difference of this work from previous [16, 17] is in a different approach for calculating the diffusion coefficient from experimental data.

It should be noted that many methods for calculating H^+ require the value of specific surface area of Ni(OH)$_2$. In some cases, the working electrode area is used instead. This is applicable if the diffusion coefficient is calculated in a series of experiments, where electrodes of the same structure are used with roughly the same load of active material. The obtained value does not correspond to the real one and is called the effective diffusion coefficient ($\overline{D}_{H^+}$). Nevertheless, such values obtained within one experiment can be used for comparative analysis.

Values of specific surface area for nickel hydroxide powders also vary over a wide range. The paper [19] lists the values of $6-150$ m^2/g (BET) for hydroxide powders synthesized via different.

For composite material containing Co-Ni(OH)$_2$/carbon spheres, the value measured by the BET was 367 m^2/g [20]. The authors found this composite to have high specific electrochemical characteristics: 959.7 F/g at a current density of 1 A/g.

The paper [21] describes the specific surface area value (477.7 m^2/g), measured by the BET, of mesoporous nickel hydroxide synthesized in the presence of a template (sodium dodecylsulfate) and urea via the hydrothermal method. Nickel oxide prepared by calcination of Ni(OH)$_2$ precipitate demonstrated a high capacity of about 124 F/g.

In another study [22], nickel hydroxide was synthesized in the form of nanoflowers, doped with boron, which demonstrated high characteristics. Its specific capacity was 2.296 F/g at a current density of 3 A/g.

As such, the listed values can vary over wider ranges, which indicates a significant influence of the synthesis method on these physico-chemical parameters, which in turn, influences the electrochemical activity of powders.

3. The aim and objectives of the study

The aim of the study is to determine the influence of the synthesis method on physico-chemical characteristics of Ni(OH)$_2$ powders: structure, morphology, proton diffusion coefficient and specific surface area. The latter two parameters are the most important for the electrochemical activity of nickel hydroxide powders. Synthesis methods that drastically differ from each other were chosen for this purpose.

To achieve the set aim, a few objectives must be accomplished:

– to precipitate Ni(OH)$_2$ powders using different methods;

– to conduct a comparative analysis of morphology and structure of prepared powders;

– to determine physico-chemical properties of powders: specific surface area and proton diffusion coefficient.

4. Material and method used in the study

Reagents and materials used in the experiments

Analytical grade reagents were used in the study. Samples used in the experiments: $Ni(OH)_2$ powder synthesized hydrolytically, nickel hydroxide co-precipitated with aluminum cations [24], industrial powder of Czech company "Bochemie" [25], and experimental industrial powder of Russian company "AIT" [26], activated with carbonate-ion. Sample labels are listed in Table 1.

Table 1

Powder labels in the study

Sample description	Hydro-lytically synthesized	Double hydroxide Ni–Al	By Czech company "Bochemie"	By Russian company "AIT"
Label	H	Ni–Al	"Bochemie"	"AIT"

Hydrolytic synthesis of $Ni(OH)_2$.

$Ni(NO_3)_2 \cdot 6H_2O$ (63 g) and urea (172 g) were dissolved in 720 ml of distilled water. The solution was transferred into a round-bottom glass flask and stirred for 6 h at 90 °C. The reaction mixture was then cooled to room temperature, the precipitate was filtered and kept in water for a day. The powder was dried at 60 °C and ground in a ceramic mortar. The dried powder was then sifted through a 70 µm sieve. The obtained powder was used in the experiments.

Synthesis of double hydroxide with aluminum cations. The sample was synthesized according to the literature [24]. Solutions were prepared based on the composition of double hydroxide $Ni_{0.8}Al_{0.2}(OH)_2(CO_3)_{0.1} \cdot 0.66H_2O$.

Structure and morphology analysis

Morphology and structure of $Ni(OH)_2$ powders used in the experiments were analyzed using: Scanning Electron Microscope (SEM) JEOL JSM-6510LV (Japan) and X-ray diffractometer DRON-3 (Russia). XRD patterns were recorded in Co-Kα monochromatic radiation.

Measurement of specific surface (S_{sp})

Specific surface area of nickel hydroxide samples was measured using the dye absorption method [27]. Methylene Blue dye was used in the experiment. The amount of absorbed dye was measured as a change in the optical density of dye solutions with nickel hydroxide powder, Fig. 2. Optical density was measured using a photoelectric colorimeter – PEC-M (Russia). Specific surface area of nickel hydroxide samples was calculated using the surface area that the absorbed Methylene Blue molecule occupies in vertical orientation – $7.5 \cdot 10^{-20}$ m^2 ($135 \cdot 10^{-20}$ m^2 in horizontal orientation).

Measurement of proton diffusion coefficient (D_{H^+})

To measure D_{H^+}, active electrode mass was prepared with different $Ni(OH)_2$ hydroxide powders, graphite, as a conductive additive, and polytetrafluoroethylene (PTFE) emulsion, as a binder.

Composition of active mass is listed in Table 2.

Active mass of each sample was pasted onto electrodes, and their cyclic voltamperometry (CV) curves were recorded using the YSE-2 cell (Fig. 3). CV-were recorded at different scan rates: 1; 2; 5; 10 mV/s, and a separate CV was recorded at 0.5 mV/s. Scan rates were recorded using the potentiostat PI-50-1.1 (Russia).

Fig. 2. Flasks of nickel hydroxide powders in methylene blue solution

Table 2

Composition of active mass

Component	Name	ω, %
Nickel hydroxide	–	74
Graphite	GAK-3	16
PTFE	F-4D	10
Σ	–	100

Fig. 3. Electrochemical cell YSE-2 for measuring the proton diffusion coefficient

Cyclic voltamperometry curves were used to determine anodic and cathodic potential peak currents; current values were plotted against the square root of scan rate. Plot angle was equal to $I/\nu^{1/2}$. This value was used in the Randles-Sevcik equation ((3), [28]) to calculate the proton diffusion coefficient in the solid phase:

$$I = 2.69 \cdot 10^5 \cdot n^{3/2} \cdot S \cdot C \cdot D^{1/2} \cdot \nu^{1/2}, \qquad (3)$$

where ν – scan rate, V/s; n – number of electrons transferred (1); S – real surface area of the electrode (mass of active material multiplied by its specific surface area), cm^2; C – maximum concentration of proton vacancies, mole/cm^2 (0.045 mole/cm^3); I – peak current, A; D – diffusion coefficient, cm^2/s.

5. Analysis and comparison of morphology and structure of powders studied in the experiment

XRD patterns of all samples used in the study are shown in Fig. 4. Analysis of XRD patterns revealed that all powders significantly differ in structure. Degree of crystallinity (size of crystals with ideal structure) and polymor-

phic form differ from each other. It can be said that samples "Bochemie" and "AIT" have larger crystal size and higher degree of crystallinity, with a smaller number of structural defects. The other two powders have a larger number of defects and are different polymorphs. This is evident from the first peak situated at 12–15° (Fig. 4, blue line), which means that these powders are α-Ni(OH)$_2$. Two industrial samples are β-Ni(OH)$_2$.
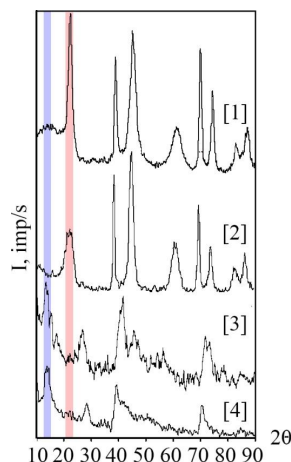
Fig. 4. Comparison of XRD patterns of Ni(OH)$_2$ powders Ni(OH)$_2$: 1 — "Bochemie"; 2 — "AIT"; 3 — Ni-Al; 4 — H

Fig. 5 shows SEM images of samples. Comparative analysis of sample morphology shows significant differences in the morphology of samples.

Sample "Bochemie" is composed of shard-like particles with microbumps on the surface of different shapes, Fig. 5, a, b.

At the same time, "AIT" sample has a platelet-like morphology, Fig. 5, d, e. Hydroxide platelets are chaotically oriented in different directions with frequent intergrowth of platelets.

Particles of Ni–Al samples have a rounded shape, upon closer examination the surface is almost uniform and dense.

Sample H shows a significantly different morphology. The surface has a lot of branches and layers.

5. 1. Comparative analysis of S_{sp} and D_{H^+} values obtained for the studied powders and their electrochemical characteristics

Two sets of CV were recorded for each sample. The first CV was recorded at a minimal scan rate of 0.5 mV/s for the study of hydroxide. The second one was recorded at various scan rates. CV for all samples are shown in Fig. 6–9, a, b.
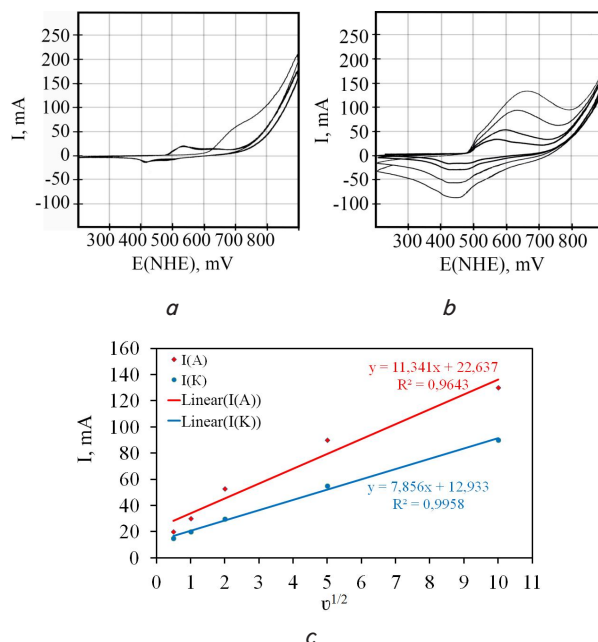
Fig. 6. CV of powder "Bochemie": a — 0.5 mV/s (5 cycles), b — 1, 2, 5, 10 mV/s, c — dependency of peak currents on the square root of scan rate

Fig. 6 shows listed dependencies for Czech powder. CV for the study of hydroxide showed the presence of one anodic and one cathodic peak. The first anodic peak is shifted significantly in comparison with the subsequent ones. Intense oxygen evolution is observed at 800–900 mV. CV recorded at different scan rates is shown in Fig. 6, b.

Fig. 5. Surface morphology of Ni(OH)$_2$ powders: a, b — "Bochemie"; c, d — "AIT"; e, f — Ni–Al; g, h — H

It can be seen that cathodic and anodic peaks grow and shift with each new scan rate. For illustration, the data from CV was used to plot the dependency of peak currents (cathodic and anodic) on the square root of scan rate, Fig. 6, *b*. The obtained dependency shows a linear character, which is characteristic for processes limited by diffusion. Slope angle was used for calculation of diffusion coefficients.
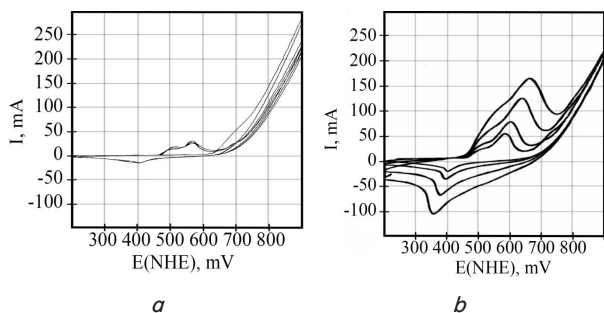
Fig. 7. CV of powder "AIT":
a — 0.5 mV/s (5 cycles), *b* — 1, 2, 5, 10 mV/s
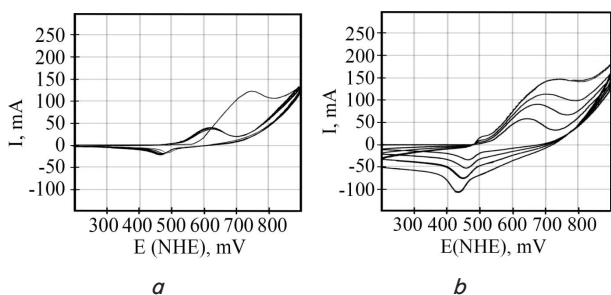
Fig. 8. CV of powder Ni—Al:
a — 0.5 mV/s (5 cycles), *b* — 1, 2, 5, 10 mV/s

Other powders demonstrated characteristics that significantly differ from each other. Differences were in both peak position and peak currents, Fig. 7–9. The lowest currents in the experiment were demonstrated by powder synthesized via hydrolysis (sample H). Sample "AIT" demonstrated the presence of two anodic peaks. It should be noted that CV of sample Ni–Al revealed high reversibility of the process (small distance between the cathodic and anodic peaks). This is the only sample for which cathodic peak position was shifted left the most.
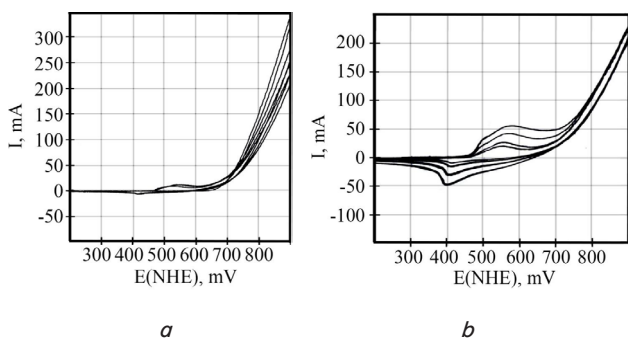
Fig. 9. CV of powder H:
a — 0.5 mV/s (5 cycles), *b* — 1, 2, 5, 10 mV/s

Calculation of diffusion coefficients requires a specific surface area of powders. These values were measured using

the dye absorption method. Measurement results are presented in Fig. 10. Sample Ni-Al has the lowest surface area, while sample H the highest. Difference between powder values is almost an order of magnitude.
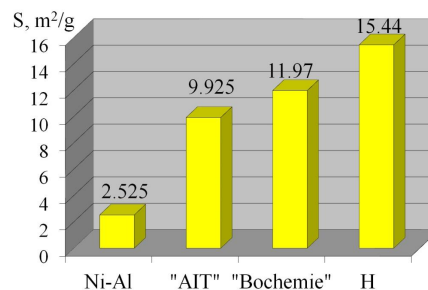
Fig. 10. Specific surface area values of powders used in the experiment

Diffusion coefficient calculated using S_{sp} values for cathodic and anodic peaks (processes) are shown in Fig. 11.

Analysis of these values allows concluding that found values differ significantly (by orders), which can significantly affect the usability of hydroxide for a specific purpose.
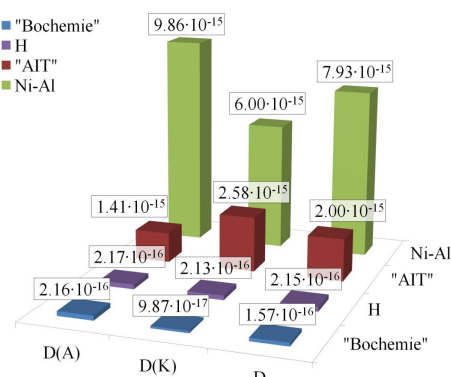
Fig. 11. H$^+$ diffusion coefficients in the solid phase, calculated using the Randles-Sevcik equation (cm^2/s): D(A) — from the anodic peak current, D(C) — from the cathodic peak current, D — average between D(A) and D(C)

It can be stated that diffusion coefficients for anodic and cathodic processes differ significantly. For sample "AIT", proton diffusion coefficient for the cathodic process is higher than that for the anodic process. For the hydrothermally prepared sample, anodic and cathodic diffusion coefficients are almost the same. For the other two samples, the anodic diffusion coefficient is higher than cathodic.

6. Discussion of the data obtained for the studied powders

Comparative analysis revealed significant structural and morphological differences of powders. It is obvious that the synthesis method affects the characteristics of the resulting compounds. The hydrothermal method and introduction of aluminum result in the formation of the α form of hydroxide. In turn, "classic" methods of hydroxide precipitation for alkaline batteries result in the β form of nickel hydroxide. Formation of β-Ni(OH)$_2$ occurs despite the presence of the carbonate ion (sample "AIT"), which should reside in the interlayer space of hydroxide. The latter should result in the

formation of the α form due to the expansion of the interlayer space. However, because there are no cations to balance the excessive negative charge of the interlayer space, the precipitation process occurs differently. Precipitation in the presence of CO_3^{2-} likely results in the formation of hydroxide and a portion of basic salt of $[Ni(OH)]_2CO_3$ type.

Powder morphology allows for qualitative evaluation of possible differences in specific surface area of different powders. For instance, hydroxide that doesn't have a branching structure, like sample Ni–Al, would have a low specific surface area. Which is supported by the fact that this sample has the lowest value of specific surface area (2.52 m^2/g). Thus, it can be said that morphology images can be used for qualitative evaluation of specific surface area. The sample prepared using the hydrothermal method (sample H) demonstrated a branched surface shape in the form of wavy intersecting planes. Obviously, such hydroxide should have a high specific surface area, which is shown by the measured value of S_{sp} – 15.44 m^2/g. It should be noted that the morphology of this sample differs significantly from other samples. This is likely related to the synthesis method, which unique in that urea hydrolysis occurs with a uniform increase of pH across the whole volume of the solution that contains Ni^{2+}. This synthesis method contrasts with others ones, in which two solutions are mixed and initial $Ni(OH)_2$ is formed on the contact boundary between the alkali solution, with a high concentration of OH^-, and the solution with nickel ions.

As expected, electrochemical characteristics are also different. All peak currents were proportional to the square root of the scan rate. It is worth to note that this dependency is linear for all powders, which is characteristic of the processes limited by diffusion. Presented facts allow concluding that the synthesis method does not affect the nature of the limiting stage. A small deviation from linearity for the anodic process can be explained by the occurrence of side reaction of oxygen evolution, which contributes to the peak current.

The obtained values of S_{sp} are within the range of the values obtained by the BET method, found in the literature. The BET method is considered the etalon for measuring S_{sp}. Nevertheless, the dye molecule is significantly larger than the nitrogen molecule and doesn't always absorb into the smallest pores of hydroxide. On the other hand, the electrochemical process is unlikely to occur in such hardly accessible places due to their high resistance. The latter is related to the small cross-section of such pores, and because the solvated molecule is larger than the nitrogen molecule. As such, the real specific surface area that is involved in the electrochemical process can be lower than that measured by the BET method. As a result, this can lead to significant errors in the calculation of diffusion coefficients, when the specific surface area is measured by absorption methods.

The obtained diffusion coefficient values are within the range of what has been found by other groups [13–18]. It is interesting that the obtained values are different not only for different powders, but also differ depending on the synthesis method. Sample "AIT" is the only sample, which has a lower anodic diffusion coefficient than cathodic ($1.41 \cdot 10^{-15}$ and $2.58 \cdot 10^{-15}$ cm^2/s respectively). For sample Ni-Al, on the opposite – cathodic proton diffusion coefficient is lower than anodic ($6 \cdot 10^{-15}$ and $9.86 \cdot 10^{-15}$ cm^2/s respectively). For the other two samples, the difference between diffusion coefficients is less pronounced, and they fall into the range of $0.98 \cdot 10^{-16} - 2.17 \cdot 10^{-16}$ cm^2/s.

The highest diffusion coefficients in the solid phase are demonstrated by powder Ni-Al, which we relate to the defective structure and presence of water in the crystal lattice. It is easier for proton to travel through defective areas and areas with admixtures and water, and through areas with bound water. Possible diffusion mechanism – H^+ jumping from one water molecule to another.

In the end, it should be pointed out that determination of diffusion coefficients in the solid phase can help in the evaluation of hydroxide application. For instance, powders with higher diffusion coefficients but lower specific surface area are more suited for slow discharge with low currents, which is typical for batteries. In turn, powders with high specific surface areas are more suited for high rate regimes with high currents, which is more typical for electrochemical supercapacitors. As such, powders Ni-Al and "AIT" are more suited for batteries, while there is a good chance that the hydroxide "Bochemie" is applicable for supercapacitors.

Mixing of different powders is also an option, which can lead to solutions for non-trivial problems.

7. Conclusions

1. To solve the set problems, precipitation of $Ni(OH)_2$ powders was carried out using different methods: hydrothermal, using urea, and precipitation of nickel-aluminum double hydroxide from a mixed salt solution.

2. Conducted comparative analysis revealed significant differences in morphology and structure of powders: samples Ni–Al and H showed the presence of α-$Ni(OH)_2$, relatively low degree of crystallinity and high number of defects. On the other hand, two industrial samples showed only the presence of β-$Ni(OH)_2$, relatively high degree of crystallinity.

3. Specific surface area values of powders were determined using the dye absorption method. The values are: Ni–Al – 2.525 m^2/g "AIT" – 9.925 m^2/g "Bochemie" – 11.97 m^2/g and H – 15.44 m^2/g. For all hydroxide samples, electrochemical characteristics and H^+ diffusion coefficients were evaluated, which lie within $9.86 \cdot 10^{-15} - 9.87 \cdot 10^{-17}$ cm^2/s.

References

1. Kotok V., Kovalenko V., Malyshev V. Comparison of oxygen evolution parameters on different types of nickel hydroxide // Eastern-European Journal of Enterprise Technologies. 2017. Vol. 5, Issue 12 (89). P. 12–19. doi: https://doi.org/10.15587/1729-4061.2017.109770

2. Kotok V., Kovalenko V., Vlasov S. Investigation of NiAl hydroxide with silver addition as an active substance of alkaline batteries // Eastern-European Journal of Enterprise Technologies. 2018. Vol. 3, Issue 6 (93). P. 6–11. doi: https://doi.org/10.15587/1729-4061.2018.133465

3. Kovalenko V., Kotok V. Definition of effectiveness of β-Ni(OH)$_2$ application in the alkaline secondary cells and hybrid supercapacitors // Eastern-European Journal of Enterprise Technologies. 2017. Vol. 5, Issue 6 (89). P. 17–22. doi: https://doi.org/10.15587/1729-4061.2017.110390

4. Kovalenko V., Kotok V. Influence of ultrasound and template on the properties of nickel hydroxide as an active substance of supercapacitors // Eastern-European Journal of Enterprise Technologies. 2018. Vol. 3, Issue 12 (93). P. 32–39. doi: https://doi.org/10.15587/1729-4061.2018.133548

5. Heterogeneous interface engineered atomic configuration on ultrathin Ni(OH)2/Ni3S2 nanoforests for efficient water splitting / Xu Q., Jiang H., Zhang H., Hu Y., Li C. // Applied Catalysis B: Environmental. 2019. Vol. 242. P. 60–66. doi: https://doi.org/10.1016/j.apcatb.2018.09.064

6. Experimental and theoretical insights into sustained water splitting with an electrodeposited nanoporous nickel hydroxide@nickel film as an electrocatalyst / Xing Z., Gan L., Wang J., Yang X. // Journal of Materials Chemistry A. 2017. Vol. 5, Issue 17. P. 7744–7748. doi: https://doi.org/10.1039/c7ta01907f

7. Soft Electrochemical Etching of FTO-Coated Glass for Use in Ni(OH)$_2$-Based Electrochromic Devices / Kotok V. A., Malyshev V. V., Solovov V. A., Kovalenko V. L. // ECS Journal of Solid State Science and Technology. 2017. Vol. 6, Issue 12. P. P772–P777. doi: https://doi.org/10.1149/2.0071712jss

8. Kotok V., Kovalenko V. A study of multilayered electrochromic platings based on nickel and cobalt hydroxides // Eastern-European Journal of Enterprise Technologies. 2018. Vol. 1, Issue 12 (91). P. 29–35. doi: https://doi.org/10.15587/1729-4061.2018.121679

9. Nickel hydroxides and related materials: a review of their structures, synthesis and properties / Hall D. S., Lockwood D. J., Bock C., MacDougall B. R. // Proceedings of the Royal Society A: Mathematical, Physical and Engineering Sciences. 2014. Vol. 471, Issue 2174. P. 20140792–20140792. doi: https://doi.org/10.1098/rspa.2014.0792

10. Structural characteristics of spherical Ni(OH)$_2$ and its charge/discharge process mechanism / Peng M., Shen X., Wang L., Wei Y. // Journal of Central South University of Technology. 2005. Vol. 12, Issue 1. P. 5–8. doi: https://doi.org/10.1007/s11771-005-0191-x

11. Effect of electrodeposition temperature on the electrochemical performance of a Ni(OH)$_2$ electrode / Wang Y.-M., Zhao D.-D., Zhao Y.-Q., Xu C.-L., Li H.-L. // RSC Adv. 2012. Vol. 2, Issue 3. P. 1074–1082. doi: https://doi.org/10.1039/c1ra00613d

12. Song Q. S., Chiu C. H., Chan S. L. I. Effects of ball milling on the physical and electrochemical characteristics of nickel hydroxide powder // Journal of Applied Electrochemistry. 2015. Vol. 36, Issue 1. P. 97–103. doi: https://doi.org/10.1007/s10800-005-9045-3

13. Structural and Electrochemical Characteristics of Sintered Nickel Electrodes / Rus E. M., Constantin D. M., Oniciu L., Ghergari L. // Croatica Chemica Acta. 1999. Vol. 72, Issue 1. P. 24–51.

14. Ten'kovcev V. V., Centner B. I. Osnovy teorii i eksplutacii germetichnih nikel'-kadmievyh akkumulyatorov. Leningrad: Energoatomizdat, Leningr. otd-nie, 1985. 96 p.

15. Motupally S. Proton Diffusion in Nickel Hydroxide Films // Journal of The Electrochemical Society. 1995. Vol. 142, Issue 5. P. 1401. doi: https://doi.org/10.1149/1.2048589

16. MacArthur D. M. The Proton Diffusion Coefficient for the Nickel Hydroxide Electrode // Journal of The Electrochemical Society. 1970. Vol. 117, Issue 6. P. 729. doi: https://doi.org/10.1149/1.2407618

17. Briggs G. W. D., Snodin P. R. Ageing and the diffusion process at the nickel hydroxide electrode // Electrochimica Acta. 1982. Vol. 27, Issue 5. P. 565–572. doi: https://doi.org/10.1016/0013-4686(82)85041-x

18. Zhang C. The Anodic Oxidation of Nickel in Alkaline Media Studied by Spectroelectrochemical Techniques // Journal of The Electrochemical Society. 1987. Vol. 134, Issue 12. P. 2966. doi: https://doi.org/10.1149/1.2100324

19. Kovalenko V., Kotok V., Bolotin O. Definition of factors influencing on Ni(OH)$_2$ electrochemical characteristics for supercapacitors // Eastern-European Journal of Enterprise Technologies. 2016. Vol. 5, Issue 6 (83). P. 17–22. doi: https://doi.org/10.15587/1729-4061.2016.79406

20. Facile preparation of a novel composite Co-Ni(OH)$_2$/ carbon sphere for high-performance supercapacitors / Jiang X., Cheng W., Hu H., Hu Y., Cao Y., Yan S. et. al. // Materials Technology. 2018. Vol. 34, Issue 4. P. 204–212. doi: https://doi.org/10.1080/10667857.2018.1548115

21. Synthesis and electrochemical properties of mesoporous nickel oxide / Xing W., Li F., Yan Z., Lu G. Q. // Journal of Power Sources. 2004. Vol. 134, Issue 2. P. 324–330. doi: https://doi.org/10.1016/j.jpowsour.2004.03.038

22. Boron-doped α-Ni(OH)$_2$ nanoflowers with high specific surface area as electrochemical capacitor materials / Yang J.-H., Wang C., Yang D., Li X., Shang P., Li Y., Ma D. // Materials Letters. 2014. Vol. 128. P. 380–383. doi: https://doi.org/10.1016/j.matlet.2014.04.170

23. Jayalakshmi M., Rao M. M., Kim K.-B. Effect of Particle Size on the Electrochemical Capacitance of α-Ni(OH)$_2$ in Alkali Solutions // International Journal of Electrochemical Science. 2006. Vol. 1, Issue 6. P. 324–333.

24. Physical and electrochemical characteristics of aluminium-substituted nickel hydroxide / Liu B., Wang X. Y., Yuan H. T., Zhang Y. S., Song D. Y., Zhou Z. X. // Journal of Applied Electrochemistry. 1999. Vol. 29, Issue 7. P. 853–858. doi: https://doi.org/10.1023/a:1003537900947

25. Nickel hydroxide powder. URL: https://www.bochemie.cz/en/materials-industrial-batteries/nickel-hydroxide/nickel-hydroxide-powder

26. Zavod avtonomnyh istochnikov toka. URL: http://www.zait.ru/

27. Tewari B. B., Thornton C. O. Use of basic Methylene Blue Dye for specific surface area measurement of metal hexacyanoferrate(II) complexes // Revista de la Sociedad Química del Perú. 2010. Vol. 76, Issue 4. P. 330–335.

28. Gorohovskaya V. I., Gorohovskiy V. V. Praktikum po elektrohimicheskim metodam analiza. Moscow: Vysshaya shkola, 1983. 191 p.